Advances in Science and Technology Research Journal, 2026, 20(1), 340–353 https://doi.org/10.12913/22998624/211036 ISSN 2299-8624, License CC-BY 4.0 Received: 2025.07.01 Accepted: 2025.09.18 Published: 2025.11.21

Influence of unsupported sleeper on static deflections of CWR track based on field investigations

Włodzimierz Andrzej Bednarek¹

¹ Institute of Civil Engineering, Faculty of Civil and Transport Engineering, Poznan University of Technology, ul.Piotrowo 5, 61-138 Poznan, Poland E-mail: wlodzimierz.bednarek@put.poznan.pl

ABSTRACT

The paper presents the results of the author's field investigation in continuous welded rail (CWR) track subjected to generated imperfection and applied static forces. During field tests the measurement system Pontos is used. In the railway track the phenomenon of unsupported sleepers (i.e. effect of hanging sleeper) is simulated and analyzed. The used author's method, making use from the measurement in the loaded track, allows for the tracking changes in railway track's work and its behavior. The obtained results significantly change the deflections and stresses in the railway track structure (especially in characteristic cross-sections: the beginning/end and the middle of the irregularity). The measurements and analyses presented in the paper show a significant changes the behavior of the loaded elements of the railway track structure (in the case of sleeper deflections even their twice increase). In the paper on the basis of simulated irregularities (contact loss between the track and ballast along its length), the measurements of rail and sleeper deflections, as well as the force transferred from the rail to the sleeper in a real jointless track are taken. For the maximum measured force, analyses are carried out to determine the change in static sleeper deflection along its length due to the contact loss between the sleeper and ballast (areas of lack of support in the under rail's cross-section). The obtained additional sleeper's deflections increase for the front of sleeper by 23.4%, for the rail's cross-section by 23% and for the middle of the sleeper by 22.7%.

Keywords: railway track irregularity simulation, hanging sleeper, unsupported sleeper, track's deflection.

INTRODUCTION

The railway track is the basic load-bearing element of the railway track structure. Its designed geometric layout ensures safe movement of rolling stocks. The most commonly used railway track structure in the world is a railway grid made of rails attached by fastening system to transversely lied sleepers, resting on a layer of ballast. A classic ballasted railway track structure is made of rails, rail bonds, sleepers and ballast. In addition, the railway track structure includes additional elements used in special cases: anticreep stops, guides in small-radius curves, extension joints and guard rails on bridges, turnouts and track crossings and railway crossings. Such a structure has not changed in principle since the beginning of the railway. The progress that has

taken place in the field of track structure construction is expressed mainly in the change in the method of connecting rails forming rail track, the change in the method of attaching rails to sleepers, the use of concrete or plastic sleepers (instead of wooden ones), and above all in the increase in the weight of individual track structure elements.

The upper surface of the track bed, the socalled railway subgrade, is the foundation on which the railway track is laid, which is the basic element of the technical infrastructure of the railway. Since the service life of the railway track is usually 20–30 years (sometimes even 50 years), it is very important to choose the right construction system, ensuring that the changing, most often increasing operational requirements are met over time.

The main tasks of the railway track bed include ensuring safe motion of vehicles on rails

and taking over dynamic impacts from the rolling stock wheels and transferring them to the subgrade. The railway track grid (rails attached to sleepers) properly supported on the railway ballast transfers the acting loads. The railway ballast cooperating with the track grid ensures the proper response of the track through:

- longitudinal resistance (e.g. to longitudinal forces, e.g. braking),
- transverse resistance (e.g. to transverse forces, e.g. steering),
- vertical resistance (e.g. to vertical forces loads from the vehicle axles).

Full contact of both the railway track and the sleeper with the ballast ensures the expected operation and behavior of the railway track structure during long-term operation (minimizes the effect of hanging sleepers or the possibility of track buckling during high temperatures). Progressive operation causes increased the values of the displacements, stresses and forces transferred between elements in the railway track structure. Therefore, further research are expected (analyses, computer simulations, field and laboratory tests) aimed at analyzing such unfavorable phenomena [1–5]. The deteriorating condition of the track and loads from trains cause further an increase in the dynamic impacts, noise and vibrations [6, 7]. The actual state of the railway track, its shape and layout, described by geometrical parameters (e.g. track's

width, twist, tilt, vertical and horizontal deformations of both rails) changes during long-term operation. The planned repairs in the railway track structure:

- regulation of a continuous welded rail (CWR) track,
- regulation of rail's dilatations,
- regulation of rails after creep,
- vertical realignment of the track (usually by balast tamping),
- horizontal realignment of the track,
- replacement of singular superstructure elements
- repair of a broken rail,
- regeneration of steel superstructure elements,
- replacement of turnout element,
- reprofiling of rails (grinding, milling, planing, padding),

are intended to extend the service life and reduce the costs of railway works.

The arising successive irregularities in the operated jointless track significantly change the working conditions of the loaded track elements [8–10]. The main cause of the track deformation is the variable support of the track on its length (e.g. the uneven settlement of the ballast [11–13] or weak subgrade). Such factors may cause a complete contact loss between the sleeper and the ballast (Figure 1).

Additionally, the arising imperfections, changes, wear and age of elements significantly

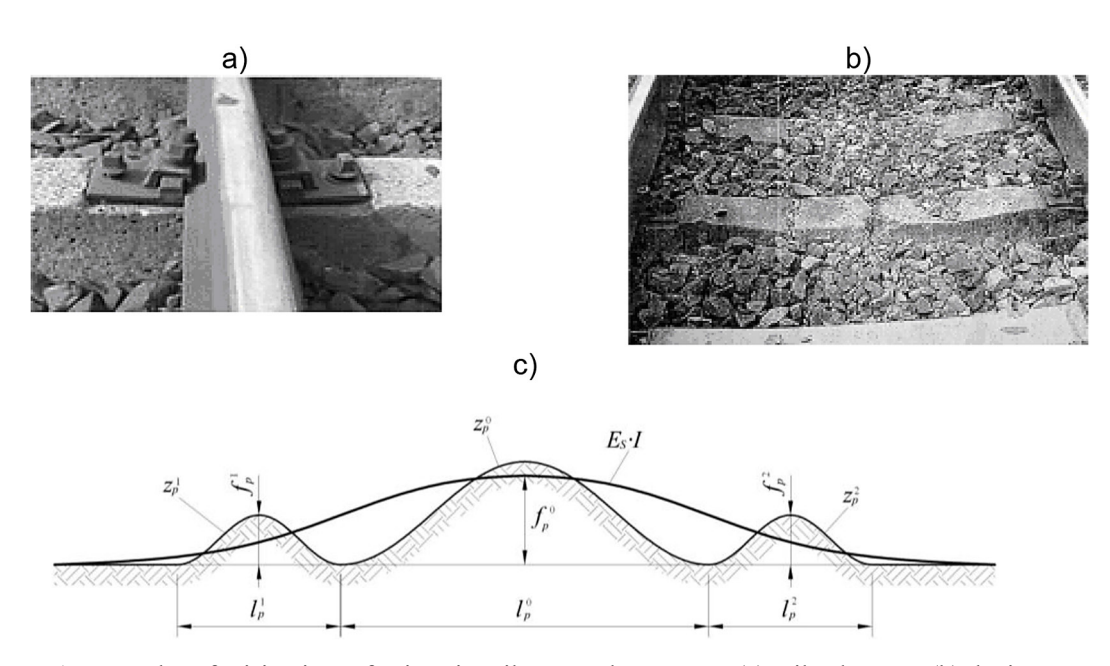


Figure 1. Examples of arising imperfections in railway track structure; (a) rail's damage; (b) the inappropriate support of sleeper in the track; (c) the arising irregularities in the railway track due to deformation of ballast (the areas of contact loss between the track and ballast) [14]

disturb the working conditions of whole railway track structure, which unfortunately lead to the successive its degradation. The arising imperfections and the influence of rolling stocks are a source of additional vehicle impacts on the railway track (Figure 1). Therefore, the further researches are necessary to know and describe the influence of arising imperfections on track behavior (e.g. problem of hanging and unsupported sleepers or contact loss between the track and ballast).

THE TRACK'S PROGRESSIVE DEGRADATION

The progressive track degradation causes the following changes in the railway track [4, 6, 15–20]:

- a) rails (especially rail's head):
- breaks, head checks, squats, break-outs,
- skid spots, indentations,
- corrugations; wear, machining errors,
- construction errors,
- b) joints and fastening:
- corrosion, breaks, indentations of plastic elements,
- missing, nut tightening,
- keeping in the sleeper,
- c) sleepers:
- breaks and squats of concrete sleepers,
- cracks of concrete sleepers,
- corrosion, rotting, indentations of wooden sleepers,
- wear of wooden sleepers at fastening,
- change of sleeper spacing,
- d) pads: brakes, missing, wear, oval holes, indentation into a sleeper,
- e) ballast and subgrade:
- ballast around sleepers and at sleepers' head,
- raveling,
- contact loss between track and ballast,
- ballast fouling (crushing, attrition),
- mud slots,
- drainage system (its patency),
- inhomogeneity of the subgrade,
- weak subgrade.

During the successive operation, the vertical forces acting on the track ($F_V = F_{V0} + F_{Vk} + F_{Vds} + F_{Vdh} + F_{Vdb} + F_{Vj}$) [21] can be divided into the following components [22]:

• F_{V0} is the static wheel force (100%),

- F_{Vk} is the quasi-static contribution in curves (0–40%),
- F_{Vds} is the dynamic contribution due to rail irregularities (0–300%),
- F_{Vdh} is the dynamic contribution due to wheel flat (0–300%),
- F_{Vdb} is the contribution due to braking (0–20%),
- F_{Vj} is the contribution due to asymmetries (0–10%) (are shown in Figure 2).

THE EFFECT OF UNSUPPORTED RAILWAY TRACK AND SLEEPERS ON THEIR BEHAVIOUR

Differential ballast settlement causes the contact loss between the sleeper bottom and the ballast (causing an "unsupported sleeper" suspended under the cooperating rail) [23]. The used granular layers (e.g. railway ballast and protecting layers) are sensitive on further progressive deformation due to the acting forces from trains (causing an accumulative deterioration of the railway track geometry). During the successive operation of a railway track, the sleepers are getting more and more unsupported or hanging [24]. According [25], the number of hanging sleepers in the track may reach up to 50% of all sleepers.

The arising unsupported railway track and sleepers in ballasted tracks are one of the frequent track defects [26]. The main reason for the

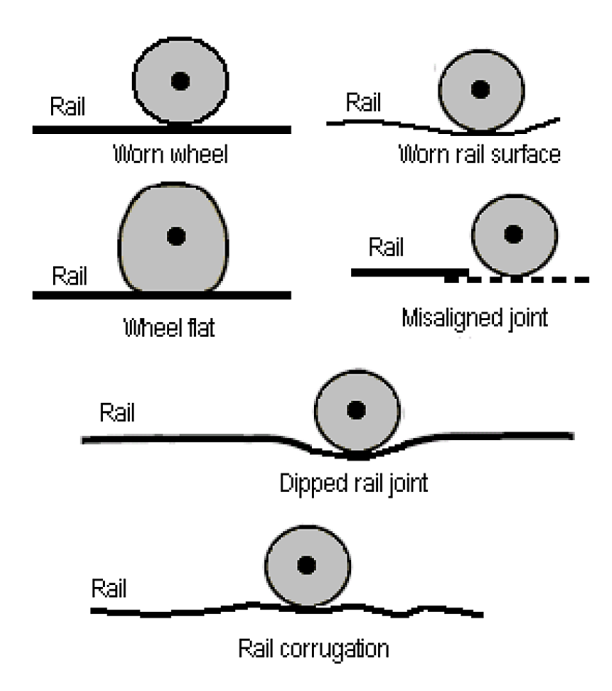


Figure 2. Various sources for impact loads in rail tracks [22]

intensive development of contact loss is the mechanics of the railway sleeper and ballast interaction (Figure 1c). Additionally, the contact loss zones cause inhomogeneous railway ballast pressure distribution between the empty area and fully supported adjacent areas [26]. In the paper [26] the mechanism of the sleeper-ballast dynamic impact in the contact loss zone is studied. It is stated, that the significant impact accelerations in this area even for lightweight slow vehicles (on the basis of measurements of rail deflections). The used model (a simple three-beam numerical model) shows that the sleeper accelerations are more than 3 times higher than the corresponding wheel accelerations. In this phenomenon the impact pointing is before the wheel enters on the impact point [26]. The ballast quasi-static loading analysis shows an increase of more than 2 times in the ballast loading in adjacent areas for long contact loss and almost full quasi-static unloading for short-length contact loss. An improved three-dimensional numerical model of railway track is used for analysis of the effects of unsupported sleepers on the dynamic behavior of track [27]. In such studies are considered the following parameters; the gap between the sleeper and the ballast, the vehicle velocity and the number of unsupported sleepers. It was stated, that consideration of sleeper compressive forces, geometry of the sleepers and an actual assumption for the sleeper-ballast contact significantly improves the precision of the results from theoretical models. In the paper [23] the experiments on 1/5-scale ballasted track models to analyze combined effects of supported and unsupported sleepers are carried out. The conducted pullout tests using panels with supported and unsupported sleepers show, that the unsupported sleepers decreasing the lateral ballast resistance. Such analyses, considering the combing effects of the sleepers support on the lateral ballast resistance, are particularly important for track's buckling considerations.

The effect of unsupported sleepers on the normal load of wheel/rail using a numerical simulation is considered in the paper [28]. The numerical research shows that the gaps between the unsupported sleepers and ballast have a significant influence on the normal load of the wheel and the rail. Also the higher velocity and the bigger gap size generate the bigger resonant frequencies of the track. Due to the arising long wavelength, the fluctuation of normal load made by the hanging sleepers does not generate the phenomenon of short-pitch corrugation of the

rail. The influence of an unsupported sleeper on the vertical bearing characteristics of Heavy-Haul Railway Ballast [29] is analyzed using a three-dimensional discrete element model (DEM) [29]. During the research a phenomenon of removing ballast particles that contacting with the bottom of the sleeper is carried out. The obtained results showed that a phenomenon of unsupported sleeper significant reduce the bearing zone of the ballast below the cooperating sleeper and also reduce the number of ballast particles that are in contact. Paper [30] presents an interesting method for estimation of the track's vertical stiffness on a basis of measured track's vertical deflections (due to various deflections of differently supported sleepers) under static railway vehicle motion along the considered track. The measurements of deflections are made on an operated railway track section for applied static axle loads of a wagon (100 kN/axle, 150 kN/axle and 200 kN/axle). On the basis of the obtained deflections the track vertical stiffness variations are estimated (with mean value: 34.98 [kN/mm] for 100 kN/axle, 43.03 [kN/mm] for 150 kN/axle and 49.96 [kN/mm] for 200 kN/axle). The main conclusion of this paper [30] is that the track response changes due to different axle loads.

The unsupported sleepers and railway tracks cause differential settlements of track superstructures, increase of dynamic loading, train-track interactions which reduce passenger comfort, safety, and maintenance cost. Cognitively interesting are analyses that consider prognostics of unsupported railway sleepers and their severity diagnostics using machine learning [31]. Such studies are important to develop new machine learning models for prognosis and diagnostics of defect severities of unsupported sleepers related to practical track inspection guidelines.

In the following points of the paper, the author shows the obtained results during field investigations and an analysis using the field research carried out (simulating the phenomenon of contact loss between the track and sleeper with ballast).

EXPERIMENTAL RESEARCH

The field tests are made at the Poznan-Franowo railway station. The main task of the field survey is to induce the intended unevenness in the railway track (by generating intended author's irregularity in the track support). Figure 3 presents the assumed

scheme of intended unevenness analyzed during field tests. During the proposed author's method of generating the intended irregularity in the track, the following activities are done:

- 1. The intended local unevenness (lowering the track by a parameter f_0 shown in Figure 3).
- 2. An intended unevenness is obtained by enabling a free move of rails and lifting the track with a screw elevator.
- 3. Next the metal plates are placed and reattaching the both rails to the sleepers.
- 4. The value of f_{θ} is gradually increased from 0 [mm] successively to 1, 2 and 3 mm.
- 5. The static load is shown in Figure 4a.
- 6. The Pontos system (Figure 4b) is used during field investigations for the static analysis [32].

The author used the Pontos system for static analysis of deflections in 3D (Figure 4b). This system makes non-contact measurements with an accuracy of 0.001 mm and a short time intervals (on the order of 0.005 [s]). The Pontos optical, mobile measurement system allows for rapid record in 3D coordinates (e.g. displacement measurements). Using the Pontos device the non-contact measures all deformations and displacements regardless of their type or structure are possible. The measurement system allows for comprehensive motion analysis, deformation detection and vibration analysis. This device allows for exceptionally precise 3D coordinates due to the use of two cameras.

During the field investigations, 12 rides with the SM-42 locomotive are done. The problem is treated as static one (the small velocity of the moving locomotive: V < 10 km/h). This made it possible to analyze the behavior of the track (for the rail and the sleeper) by measuring the deflections of both the rail itself and the sleeper. The tests are carried out on a concrete sleeper.

The changes in a real track behavior during field tests are visible under the applied loads. The obtained graphs presented in the paper and table present the proper parameters for the description of the static behavior of the CWR track as a beam resting on an elastic foundation due to its intended unevenness. The author paid special attention

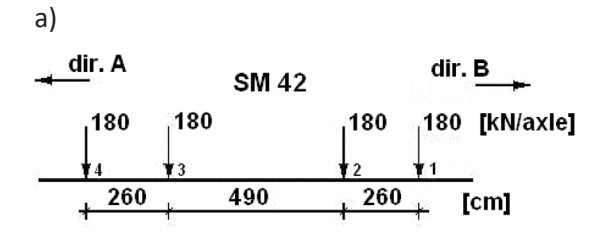




Figure 4. The measuring equipment during field tests; (a) adopted load scheme (locomotive SM-42-448); (b) a Pontos system used to record measurements

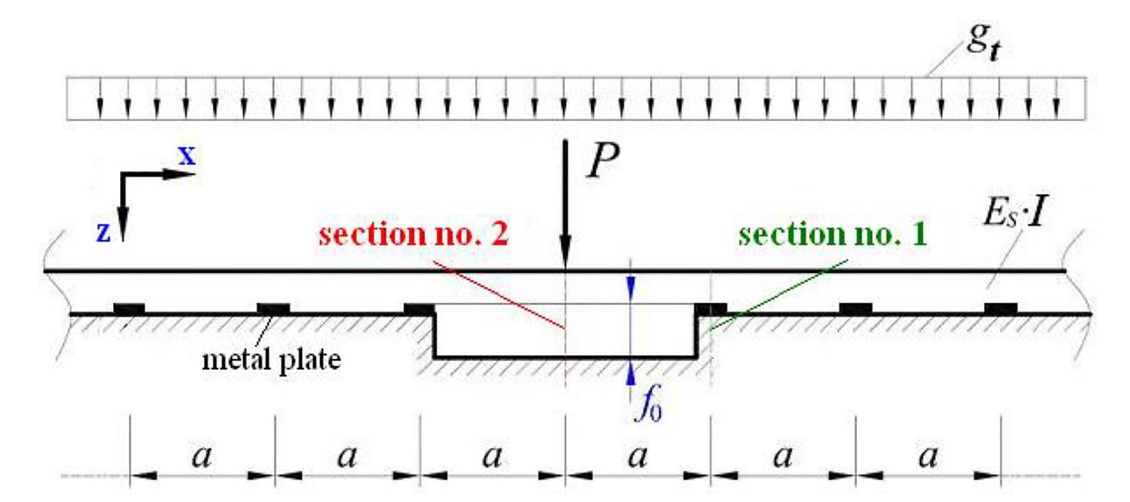


Figure 3. A scheme of induced irregularity in a railway track [author's scheme]. f_0 – an irregularity induced in railway track structure [mm], P – an applied static force [MN] (P=90 [kN/wheel]), E_s : I – a track's stiffness in vertical plane [MNm²] (E_s : I = 3.82 [MNm²]), g_t – the track's weight [MN/m] (g_t = 0.0022 MN/m), a – a spacing of the sleepers [m] (a = 0.60 m)

to the presentation of the obtained dependencies and parameters for engineering analyses.

THE OBTAINED DEFLECTIONS OF THE RAIL AND THE RAILWAY SLEEPER

During the field tests, the following parameters and values are measured for the next 4 axles of the SM-42 locomotive (for sections no. 1 and no. 2)

- the rail's and sleeper's deflections under a applied load
- the rail's stresses under a applied load
- the force transferred from the rail to the sleeper as a result of intended irregularity.

To describe the measurements obtained during the tests (deflections of both the rail and the sleeper), the following function (calculated by the Levenberg-Marquardt's method) is used:

$$z_i^n(f_0) = a \cdot (f_0)^b + c \tag{1}$$

where: f_0 – the value of f_0 gradually increased from 0 [mm] to 1, 2 and 3 [mm] in the cross-section no. 2 in [mm], a, b, c – the constants obtained from the results of field tests, i – a described section no. 1 or no. 2 (Figure 3), n – the rail's or the sleeper's deflection.

Therefore, the deflections of the rail and sleeper are described in the following form:

- the rail's deflection under a applied load: $z_i^r(f_0)$
- the sleeper's deflection at its end under a applied load: $z_i^s(f_0)$ where: i a considered section no. 1 or no. 2 (shown in Figure 3).

Figure 5 shows the measured deflection of the rail and the sleeper during field investigations in cross-section no. 1 and in cross-section no. 2 in the railway track. This figure make it possible to assess the scale of changes in considered cross-sections.

ANALYSIS OF THE MEASURED DEFLECTIONS

As can be seen in Table 1 the maximum deflection for rail and sleeper arises in the case, when the successive forces are applied in section no.2. The increase in the deflection of the rail is

shown in Figure 6. The forces acting in section no. 1 causes also important deflections in section no. 2 (Figure 6a). With an irregularity $f_0 = 3.5$ [mm] in section no. 2 (Figure 3) the static forces from the locomotive are not sufficient for the contact of the rail and sleeper in this section.

The described changes in deflection lead to changes in the stresses of the rail. Figure 7 shows the changes in the stress values for sections no. 2 and no. 1 (a scheme shown in Figure 3) obtained from the measurements (the extensometer LY41-20/120 on the rail foot). As can be seen in Figure 7, according to the scheme in Figure 3, the generated track irregularity changes the deflections, and also causes a change in the value of stresses in the foot of the rail, both for section no. 1 and no. 2. In section no. 2 a large influence of the induced irregularity on the behaviour of the railway track is observed. The increasing deflection of the rail, depending on the generated irregularity f_0 , (from 0 mm to 3 mm) causes an increase of stresses in the rail from 58.478 MPa up to 75.561 MPa, i.e. by 29.22%.

In the next point, using the measured maximum force value, calculations are made of the influence of variable sleeper support (in the under rail section) on its deflections.

DEFLECTIONS OF THE CONCRETE SLEEPER DUE TO CONTACT LOSS WITH THE BALLAST IN THE UNDER RAIL'S CROSS-SECTION

During the railway track's operation, the ballast is gradually displaced in the under rail's cross-section (Figure 1b). Hence, using the value of the force measured during field tests (Figure 9a), the change in the sleeper deflection along its length is analyzed. The foundation elasticity matrices (FEM) are used to analyze the sleeper behavior, which take into account both the reaction of the ground (ballast) and the interactions transferred by the beam resting on its foundation [33]. Each element of the discretized sleeper transfers the load to the ballast, and the reaction depends on its modulus of elasticity, as well as the width of the given element. The sleeper is divided into 9 parts (where the values: x_2 , x_3 , x_7 and x_8 are the considered ballast loosening areas) and into 80 finite elements (each with a length of 0.03125 m), as shown in Figure 8. The changes in the value of

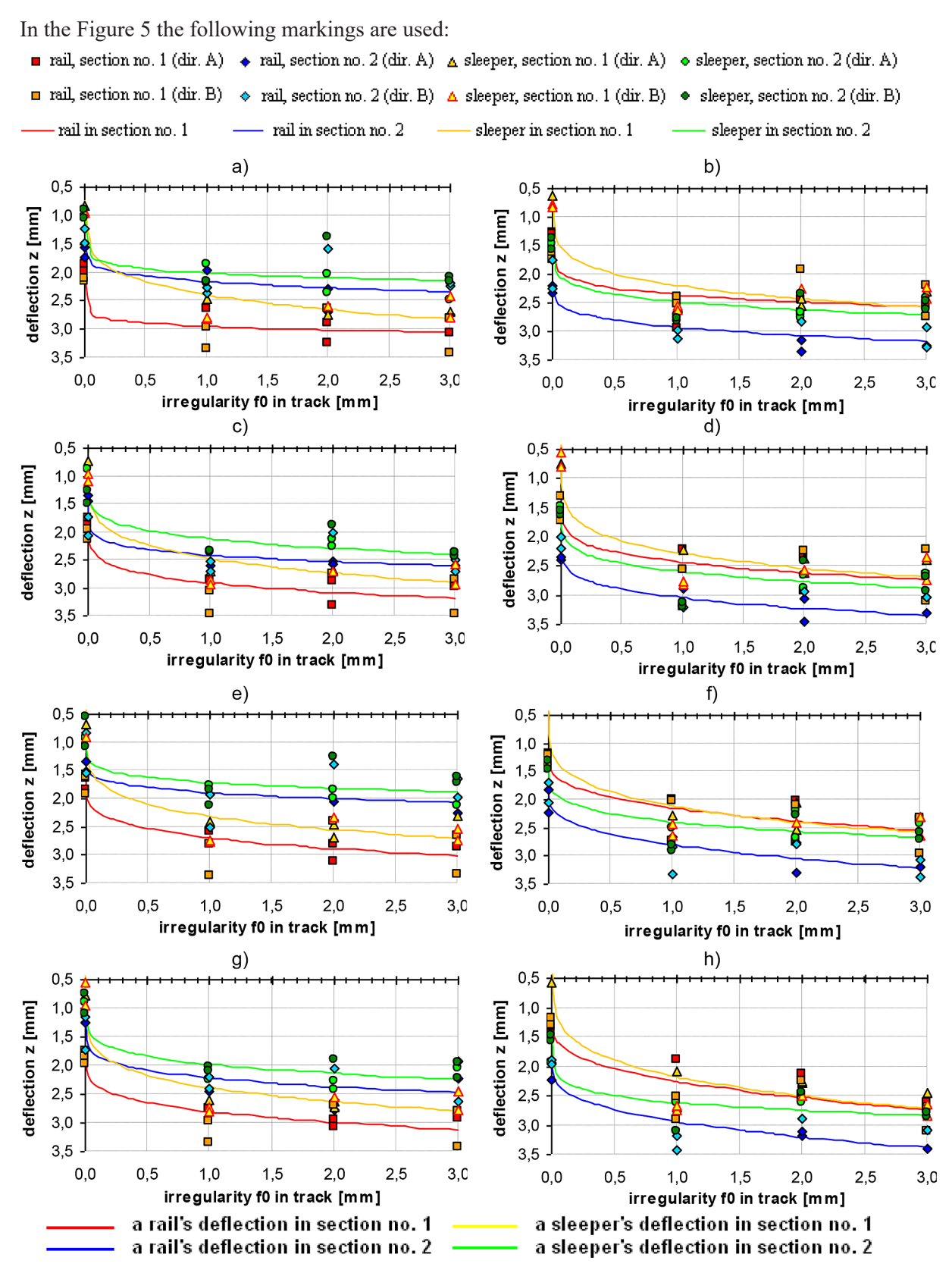


Figure 5. The rail's and the sleeper's deflections due to induced uneveness in the railway track (axle load no. 1 and no. 2 for the four axles of the SM-42 locomotive); a) acting force from 1 axle(axle load no. 1 in cross-section no. 1); b) acting force from 1 axle (axle load no. 1 in cross-section no. 2); c) acting force from 2 axle (axle load no. 2 in cross-section no. 2); e) acting force from 3 axle (axle load no. 3 in cross-section no. 1); f) acting force from 3 axle (axle load no. 3 in cross-section no. 2); g) acting force from 4 axle (axle load no. 4 in cross-section no. 1) h) acting force from 4 axle (axle load no. 4 in cross-section no. 2)

In the Table 1 the experimental values of rail and sleeper deflections in a considered section under the influence of forces from all locomotive axles are given.

Table 1. The rail's and sleeper's deflection in section no.1 and no. 2 for the succeeding axles of the SM-42 locomotive

Table 1. The	ran s and sleeper's defle	Acting force fro		es of the Sivi-42 locomotiv	
		(axle load no. 1 in cros		/	
A track's irregularity	$z_1^r(f_0) = 0.92345 \cdot (f_0)^{0.09336} + 2.02658$			$z_1^s(f_0) = 1,67416 \cdot (f_0)^{0.21019} + 0,71823$	
	$z_2^r(f_0) = 0,66469 \cdot (f_0)^{0.21692} + 1,4994$		$z_2^s(f_0) = 1,01771 \cdot (f_0)^{0.11213} + 0,99063$		
f ₀ [mm]	A rail's deflection In section no. 1	A rail's deflection In section no. 2	A sleeper's deflection In section no. 1	A sleeper's deflection In section no. 2	
	$z_1^r(f_0)$ [mm]	$z_2^r(f_0)$ [mm]	$z_1^s(f_0)$ [mm]	$z_2^s(f_0)$ [mm]	
1	2	3	4	5	
0	2.027	1.499	0.718	0.991	
1	2.949	2.164	2.392	2.008	
2	3.012	2.272	2.655	2.091	
3	3.051	2.343	2.827	2.142	
		Acting force fro (axle load no. 1 in cros			
A track's irregularity	$z_1^r(f_0) = 1,1602 \cdot (f_0)^{0,1524} + 1,1971$		$z_1^s(f_0) = 1,6593 \cdot (f_0)^{0.1889} + 0,5368$		
	$z_2^r(f_0) = 0.8003 \cdot (f_0)^{0.2407} + 2.1288$		$z_2^s(f_0) = 1,2179 \cdot (f_0)^{0.1561} + 1,2605$		
	A rail's deflection In section no. 1	A rail's deflection In section no. 2	A sleeper's deflection In section no. 1	A sleeper's deflection In section no. 2	
<i>f</i> ₀ [mm]	$z_1^r(f_0)$ [mm]	$z_2^r(f_0)$ [mm]	$z_1^s(f_0)$ [mm]	$z_2^s(f_0)$ [mm]	
1	2	3	4	5	
0	1.197	2.129	0.537	1.259	
1	2.357	2.929	2.196	2.478	
2	2.487	3.074	2.428	2.618	
3	2.569	3.171	2.579	2.706	
		Acting force fro (axle load no. 1 in cros			
A track's	$z_1^r(f_0) = 1,1602 \cdot (f_0)^{0.1524} + 1,1971$		$z_1^s(f_0) = 1,6593 \cdot (f_0)^{0.1889} + 0,5368$		
irregularity	$z_2^r(f_0) = 0.8003 \cdot (f_0)^{0.2407} + 2.1288$		$z_2^s(f_0) = 1,2179 \cdot (f_0)^{0,1561} + 1,2605$		
	A rail's deflection In section no. 1	A rail's deflection In section no. 2	A sleeper's deflection In section no. 1	A sleeper's deflection In section no. 2	
<i>f</i> ₀ [mm]	$z_1^rig(f_0ig)$ [mm]	$z_2^r(f_0)$ [mm]	$z_1^s(f_0)$ [mm]	$z_2^s(f_0)$ [mm]	
1	2	3	4	5	
0	1.197	2.129	0.537	1.259	
1	2.357	2.929	2.196	2.478	
2	2.487	3.074	2.428	2.618	
3	2.569	3.171 Acting force fro	2.579	2.706	
		(axle load no. 2 in cros	s-section no. 1)		
A track's irregularity	$z_1^r(f_0) = 1,1741 \cdot ($			$(f_0)^{0.2017} + 0.7219$	
ogularity	$z_2^r(f_0) = 1,0235 \cdot (f_0)^{0.1495} + 1,3963$			$(f_0)^{0.2245} + 1,1202$	
f [mm]	A rail's deflection In section no. 1	A rail's deflection In section no. 2	A sleeper's deflection In section no. 1	A sleeper's deflection In section no. 2	
<i>f</i> ₀ [mm]	$z_1^r (f_0)$ [mm]	$z_2^r(f_0)$ [mm]	$z_1^s(f_0)$ [mm]	$z_2^s(f_0)$ [mm]	
1	2	3	4	5	
0	1.733	1.396	0.722	1.121	
1	2.907	2.421	2.473	2.124	
2	3.075	2.532	2.736	2.293	
3	3.184	2.602	2.907	2.404	

		Acting force			
	$z_{i}^{r}(f_{i}) = 1.0323.0$	(axle load no. 2 in c $f_{.}$) ^{0,2319} +1.4024		$(f_{\rm c})^{0.1771} + 0.3868$	
A track's irregularity	$z_1^r(f_0) = 1,0323 \cdot (f_0)^{0.2319} + 1,4024$ $z_2^r(f_0) = 0.8888 \cdot (f_0)^{0.2669} + 2,1549$			$z_1^s(f_0) = 1,9002 \cdot (f_0)^{0.1771} + 0,3868$ $z_2^s(f_0) = 1,1621 \cdot (f_0)^{0.1925} + 1,4373$	
	A rail's deflection In section no. 1	A rail's deflection In section no. 2	A sleeper's deflection In section no. 1	A sleeper's deflection In section no. 2	
<i>f</i> ₀ [mm]	$z_1^r(f_0)$ [mm]	$z_2^r(f_0)$ [mm]	$z_1^s(f_0)$ [mm]	$z_2^s(f_0)$ [mm]	
1	2	3	4	5	
0	1.402	2.155	0.387	1.437	
1	2.435	3.044	2.287	2.599	
2	2.615	3.224	2.535	2.765	
3	2.734	3.347	2.695	2.873	
		Acting force (axle load no. 2 in c			
A track's irregularity	$z_1^r(f_0) = 1,0323 \cdot (f_0)^{0.2319} + 1,4024$		$z_1^s(f_0) = 1,9002$	$z_1^s(f_0) = 1,9002 \cdot (f_0)^{0.1771} + 0,3868$	
	$z_2^r(f_0) = 0.8888 \cdot (f_0)^{0.2669} + 2.1549$		$z_2^s(f_0) = 1,1621$	$z_2^s(f_0) = 1,1621 \cdot (f_0)^{0.1925} + 1,4373$	
	A rail's deflection In section no. 1	A rail's deflection In section no. 2	A sleeper's deflection In section no. 1	A sleeper's deflection In section no. 2	
<i>f</i> ₀ [mm]	$z_1^r(f_0)$ [mm]	$z_2^r(f_0)$ [mm]	$z_1^s(f_0)$ [mm]	$z_2^s(f_0)$ [mm]	
1	2	3	4	5	
0	1.402	2.155	0.387	1.437	
1	2.435	3.044	2.287	2.599	
2	2.615	3.224	2.535	2.765	
3	2.734	3.347	2.695	2.873	
		Acting force (axle load no. 3 in c			
A track's	$z_1^r(f_0) = 0.9096 \cdot (f_0)^{0.3353} + 1.2308$		$z_1^s(f_0) = 1,9354$	$z_1^s(f_0) = 1,9354 \cdot (f_0)^{0,1998} + 0,1741$	
irregularity	$z_2^r(f_0) = 0.8822 \cdot (f_0)^{0.3546} + 1.9148$		$z_2^s(f_0) = 1,2239$	$z_2^s(f_0) = 1,2239 \cdot (f_0)^{0,1841} + 1,1716$	
	A rail's deflection In section no. 1	A rail's deflection In section no. 2	A sleeper's deflection In section no. 1	A sleeper's deflection In section no. 2	
<i>f</i> ₀ [mm]	$z_1^r(f_0)$ [mm]	$z_2^r(f_0)$ [mm]	$z_1^s(f_0)$ [mm]	$z_2^s(f_0)$ [mm]	
1	2	3	4	5	
0	1.231	1.915	0.174	1.172	
1	2.139	2.797	2.111	2.396	
2	2.378	3.043	2.397	2.562	
3	2.546	3.217 Acting force		2.671	
	-r(f) 10055 ((axle load no. 4 in c		$(f_0)^{0.2275} + 0.2473$	
A track's irregularity	$z_1^r(f_0) = 1,0055 \cdot (f_0)^{0.3529} + 1,2524$ $z_2^r(f_0) = 0,9821 \cdot (f_0)^{0.3381} + 1,9594$			$(f_0)^{0.1661} + 1,4894$	
	A rail's deflection In section no. 1	A rail's deflection In section no. 2	A sleeper's deflection In section no. 1	A sleeper's deflection In section no. 2	
f ₀ [mm]	$z_1^r(f_0)$ [mm]	$z_2^r(f_0)$ [mm]	$z_1^s(f_0)$ [mm]	$z_2^s(f_0)$ [mm]	
1	2	3	4	5	
0	1.252	1.959	0.247	1.489	
1	2.258	2.941	2.176	2.615	
2	2.537	3.197	2.505	2.752	
3	2.734	3.375	2.723	2.841	

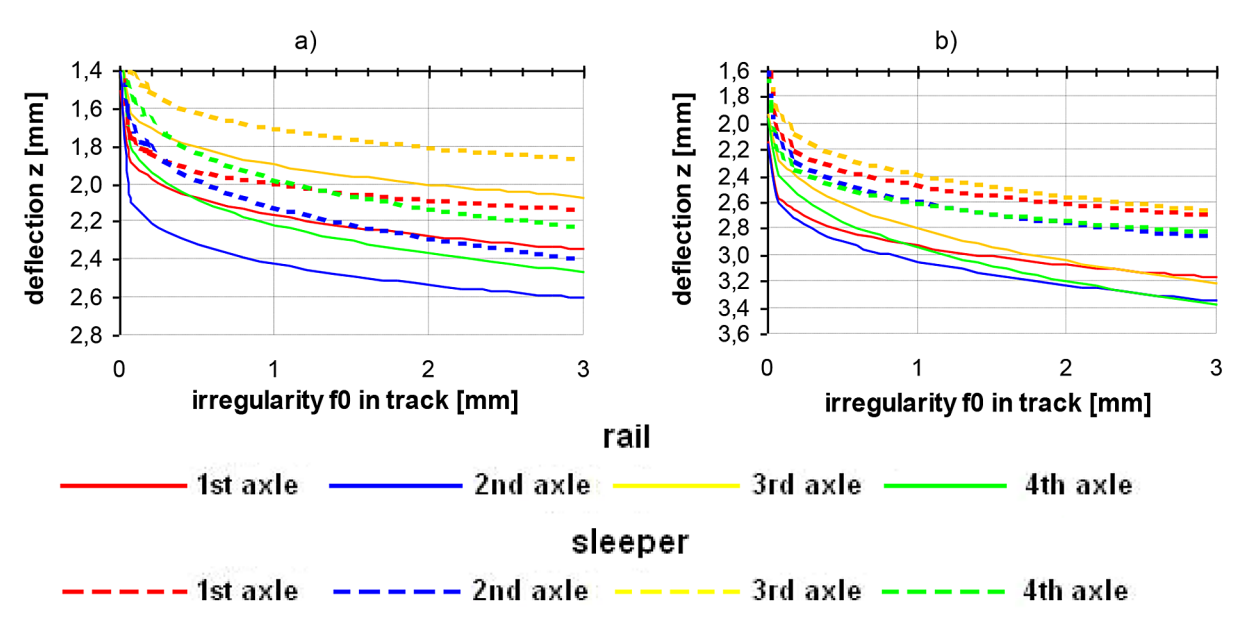


Figure 6. The rail's and sleeper's deflections for the succeeding axles of the SM-42 locomotive; a) forces in section no. 1 – changes in section no. 2; b) forces in section no. 2 – changes in section no. 2

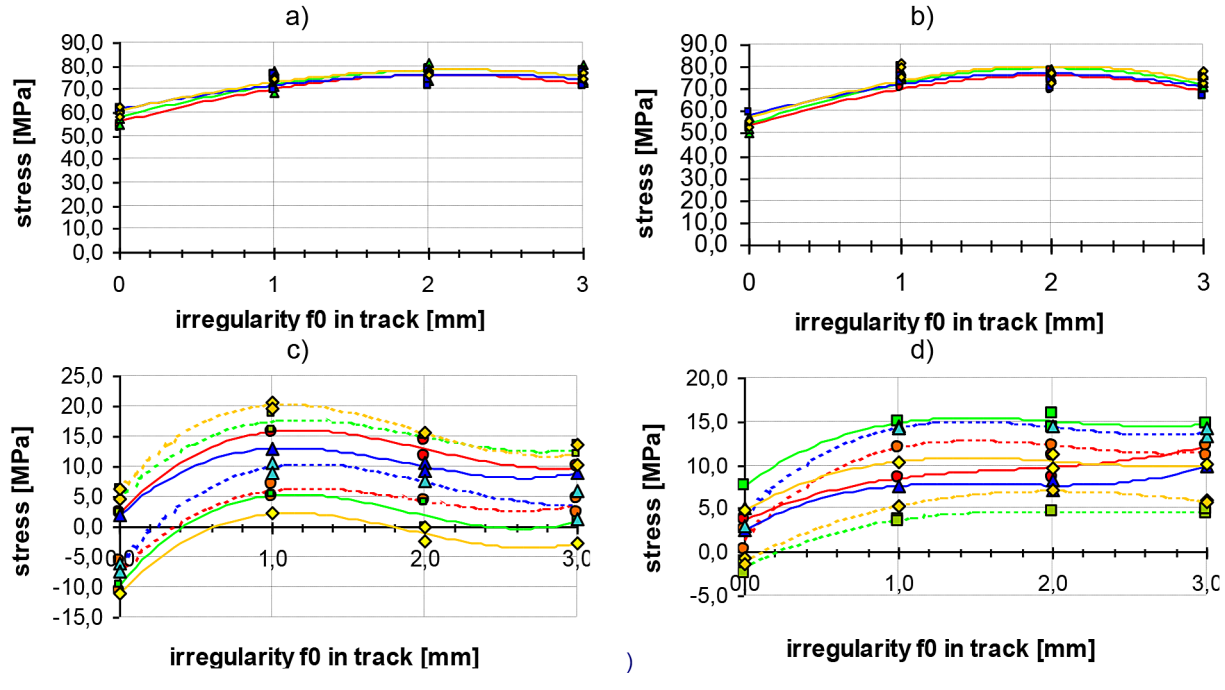


Figure 7. The changes in rail stresses on the value of f_0 induced irregularity in the railway track (the loads from the locomotive's succeeding axles); a) a stress in the rail in cross-section no. 2 - a acting force in cross-section no. 2 (the succeeding axles of locomotive); b) a stress in the rail in cross-section no. 1 - a acting force in cross-section no. 1 (the succeeding axles of locomotive); c) a stress in the rail in cross-section no. 2 - a acting force in cross-section no. 1 (the succeeding axles of locomotive); d) a stress in the rail in cross-section no. 1 - a acting force in cross-section no. 2 (the succeeding axles of locomotive)

the acting force transferred from the rail to the cooperating railway sleeper are clearly visible as a further consequence of the unevenness of the track caused by f_0 (mm) (as shown in Figure 9a). Due to the unevenness in the track (diagram in

Figure 3), the value of the force acting from the rail to the cooperating sleeper changes – in cross-section no. 2 (from 45.094 kN to 2.351 kN). For this maximum value Q = 45.094 kN the following analyses and calculations are made:

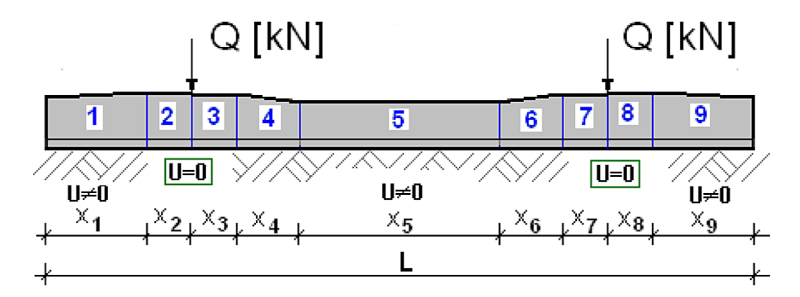


Figure 8. The assumed scheme of the considered support discontinuities, Q – force transferred from the rail to the sleeper

- 1) Identification of sleeper's foundation parameter (U = 22.836 MPa).
- 2) Assumed data for calculations: sleeper's mass 260 kg ($q_b = 1.0202 \cdot 10^{-3}$ MN/m); length of sleeper l = 2.5 m; sleeper's width b = 0.3 m; sleeper's stiffness EI = 3.8286 MNm² and sleepers spacing a = 0.6 m.
- 3) Contact loss between the sleeper and foundation (ballast) from 0 to 0.25 m (the lengths: x_2, x_3, x_7 and x_8 Figure 8).
- 4) Sleeper's deflection due to contact loss (for the front of sleeper, under rail's cross-section and in the middle of the sleeper shown in Figure 9b).

DISCUSSION

The tests carried out allow for the analysis of deflections in cross-sections no. 1 and no. 2

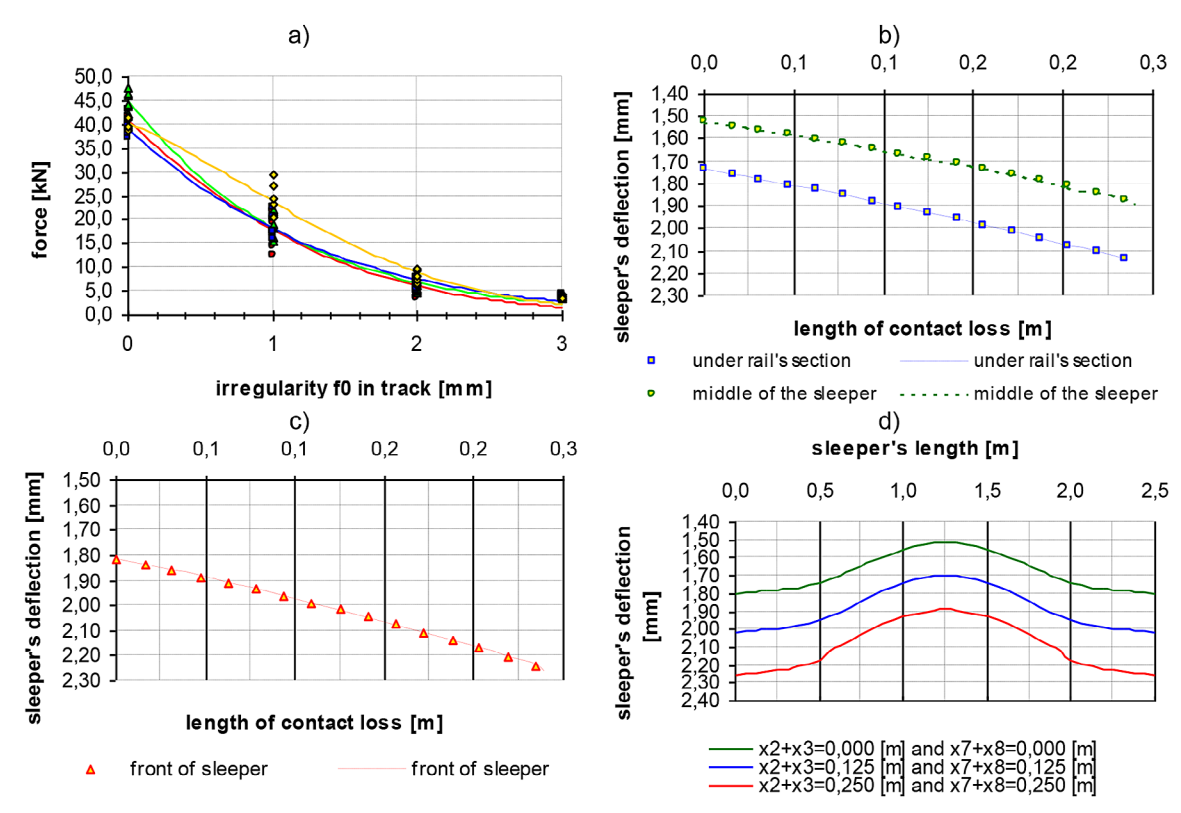


Figure 9. The force transferred from rail to sleeper and sleeper's deflection; a) the measured force transferred from the rail to the railway sleeper (the KMR200 HBM indicator installed in the sole plate) as a result the f0 value of irregularity generated in the railway track in section no. 2 (the loads from the locomotive's succeeding axles; the scheme from Figure 3 – the site investigations); b) sleeper's deflection (under rail's cross-section and middle of the sleeper) due to contact loss between the sleeper and ballast; c) maximum sleeper's deflection (from the front of sleeper) due to contact loss between the sleeper and ballast; d) sleeper's deflection along the its length due to contact loss; where the lengths: x_2 , x_3 , x_4 and x_8 are shown Figure 8

(Figure 5). As can be clearly seen in the figures (especially in Table 1), the gaps of f_0 irregularity induced in the track significantly change the work of loaded elements of the railway track structure. Particularly in the considered cross-section no. 2, one can observe a large impact of these deformations on the work of the railway track. And so:

- for the scheme in Figure 3, in the lack of irregularity in the track ($f_0 = 0$ mm), the rail's deflection is about 2 mm (e.g. under the load of 1 axle of the locomotive, the value is 2.129 mm, for 2 axle is 2.155 mm] for 3 axle is 1.915 mm; for 4 axle is 1.959 mm);
- with $f_0 = 3$ mm, the rail's deflection increases to the value of 3.171 mm for 1 axle (i.e. by 48.94%); for 2 axle by 55.31%; for 3 axle by 67.98% and for 4 axle up to 72.28%;
- the sleeper's deflection increases e.g. from 1.437 mm to 2.873 mm for 2 axle (i.e. up to 99.93%).

As can be clearly seen in the Figure 6 the generated gaps of f_0 irregularity induced in the track significantly change the work of loaded elements of the railway track structure. In the paper [26] the variable value of force transferred from the sleeper to the ballast is analyzed (from 30 kN to 60 kN). The value of the acting force measured by the author is 45.094 kN. Using the value of this measured force transferred from rail onto sleeper (Q = 45.094 kN) the numerical analysis is carried out (with considered support discontinuities). The influence of the lack of contact in the rail's crosssection is noticeable (in the obtained deflection values shown in Figure 9b and Figure 9c). For the cases shown in Figure 8, the obtained sleeper's deflection increases for the front of sleeper from 1.814 mm to 2.238 mm (by 0.424 mm), for the rail's cross-section from 1.738 mm to 2.139 mm (by 0.401 mm) and for the middle of the sleeper from 1.525 mm to 1.871 mm (by 0.346 mm). For the cases considered in [29] for the analyzed sleeper in the area of contact loss with the ballast for the force value of 45 kN, the increase in deflection from 0.29 mm to 0.34 mm]is obtained. The consequence of the contact loss between the sleeper with the ballast, in addition to the change in deflections, is a change in the values of bending moments on the length of sleeper (especially in under rail's section and in the middle of the sleeper) [14, 27].

CONCLUSIONS

Based on the defections tests carried out with static loading on sleepers hanging effect, the following conclusions can be drawn:

- A problem of the work of unsupported sleepers is important for both simulations and measurements, as well as the behavior of the railway track itself.
- The obtained dependences (deflections of the rail and the sleeper, stresses in rail and transferred force on sleeper) and graphs due to induced irregularity are presented.
- It is found out that the induced irregularity with an irregularity at value f_0 (from 0 to 3 mm) in the track significantly changes the work of the loaded elements of the railway track structure (increase in rail deflections up to approx. 72.28% and sleeper up to 99.93%). As a shown, with an irregularity $f_0 = 3.5$ mm in cross-section no. 2 the acting static forces from the locomotive are not able to ensure the full contact between the sleeper and ballast in this section.
- The resulting contact loss also causes an additional unfavorable phenomenon crushing, attrition and raveling of the ballast, especially in cross-section no. 2, which leads to the further progressive degradation of the whole railway track structure.
- The induced track irregularity changes the deflections, and thus causes a change in the value of force transferred on sleeper both for cross-section no. 1 and cross-section no. 2. For the obtained maximum value of force the analyses and calculations for sleeper due to contact loss with ballast in the under rail's cross-section are presented. The main consequence of such changes in the contact of the sleeper with the ballast is an increase in deflections in the front of the sleeper.

Acknowledgements

The author would like to thank the PKP Polish Railway Lines Poznan-Franowo for helping during the experimental setup and the site surveys. The research was financially supported by the Statutory Activity 0413/SBAD/6602, Poznan University of Technology, Faculty of Civil and Transport Engineering, Institute of Civil Engineering, Division of Bridges and Railway Engineering, 5 Piotrowo Street, 60-965 Poznan, Poland.

REFERENCES

- Abadi T., Le Pen L., Zervos A., Powrie W. Improving the performance of railway tracks through ballast interventions. Proceedings of the Institution of Mechanical Engineers, Part F: Journal of Rail and Rapid Transit, 2018; 232(2): 337–355. https://doi.org/10.1177/0954409716671545
- Sol-Sánchez M., Moreno-Navarro F., Rubio-Gámez M.C. The use of elastic elements in railway tracks: A state of the art review. Construction and Building Materials, 2015; 75: 293–305. https://doi.org/10.1177/0954409716671545
- 3. Bednarek Wł. Wybrane kierunki współczesnych innowacyjnych rozwiązań w drogach kolejowych (The chosen trends of present innovative solutions in railroads). Przegląd Budowlany 2/2025: 73–77. https://doi.org/10.5604/01.3001.0055.0983
- Bednarek W. Wybrane rozwiązania zwiększające trwałość podsypki tłuczniowej eksploatowanej nawierzchni kolejowej (Selected solutions increasing durability of breakstone ballast in operated railway track structure). Materiały Budowlane, 10/2023; 2–6. https://doi.org/10.15199/33.2023.10.09
- 5. Milne D., Le Pen L., Watson G., Thompson D., William Powrie W., Hayward M., Morley S. Monitoring and repair of isolated trackbed defects on a ballasted railway. Transportation Geotechnics, 2018; 17: 61–68. https://doi.org/10.1016/j.trgeo.2018.09.002
- Abu Sayeed M., Shahin M. A. Three-dimensional numerical modelling of ballasted railway track foundations for high-speed trains with special reference to critical speed. Transportation Geotechnics, 2016; 6: 55–65. https://doi.org/10.1016/j.trgeo.2016.01.003
- Liu G., Li P., Wang P., Liu J., Xiao J., Chen R., Wei X. Study on structural health monitoring of vertical vibration of ballasted track in high-speed railway. Journal of Civil Structural Health Monitoring, 2021; 11: 451–463. https://doi.org/10.1007/ s13349-020-00460-x
- 8. Bowe C.J., Mullarkey T.P. Wheel-rail contact elements incorporating irregularities. Advances in Engineering Software, 2005; 36(11–12): 827–837. https://doi.org/10.1016/j.advengsoft.2005.03.026
- 9. Iwnicki S.D., Bevan A.J. Damage to railway wheels and rails: A review of the causes, prediction methods, reduction and allocation of costs. The International Journal of Railway Technology, 2012; 1(1): 121–146. https://doi.org/10.4203/ijrt.1.1.6
- Zaker J.A, Xia H, Fan J.J. Dynamic response of train-track system to single rail irregularity. Latin American Journal of Solids and Structures, 2009; 6(2): 89–104.
- 11. Guerrieri M., Parla G. A new high-efficiency procedure for aggregate gradation determination of the

- railway ballast by means image recognition method. Archives of Civil Engineering, 2013; LIX(4): 469–482. https://doi.org/10.2478/ace-2013-0025
- 12. Bednarek Wł. An influence of a generated track intentional irregularity on a static work of a railway track, Archives of Civil Engineering. 2021; LXVII(1): 81–97. https://doi.org/10.24425/ace.2021.136462
- 13. Li D., Selig E.T. Evaluation of Railway Subgrade Problems. Transportation Research Record 1489.
- 14. Bednarek W. Full-Scale Field Experimental Investigation on the Intended Irregularity of CWR Track in Vertical Plane. Energies, 2021; 14(7477): 1–29. https://doi.org/10.3390/en14227477
- 15. Jing G., Luo Q., Wang Z., Shen Y. Micro-analysis of hanging sleeper dynamic interactions with ballast bed. Journal of Vibroengineering. 2015; 17(1): 444–454.
- 16. Ishida M. The progress mechanism of track geometrical irregularity focusing on hanging sleepers. International Journal of Railway Research, 2015; 2(1): 15–23. http://ijrare.iust.ac.ir/article-1-48-en.html
- 17. Karttunen K. Influence of rail, wheel and track geometries on wheel and rail degradation. Sweden, 2015.
- 18. Larsson D. A study of the track degradation process related to changes in railway traffic. Luleå University of Technology, Sweden, 2004. urn: urn:nbn:se:ltu:diva-26572, diva id: diva2:999738
- 19. Paixao A.L.M. Transition zones in railway tracks. An experimental and numerical study on the structural behaviour. Doctor's thesis, Portugal, Porto, 2014. https://hdl.handle.net/10216/99269
- Varandas J.N., Hölscher P., Silva Manuel A.G. Dynamic behaviour of railway tracks on transitions zones. Computers&Structures, 2011; 89(13–14): 1468–1479. https://doi.org/10.1016/j.compstruc.2011.02.013
- Bahrekazemi M. Train-induced ground vibration and its prediction, PhD thesis, Royal Institute of Technology, Stockholm, 2004.
- 22. Nimbalkar S., Dash S.K., Indraratna B. Performance of ballasted track under impact loading and applications of recycled rubber inclusion. Geotechnical Engineering Journal of the SEAGS & AGSSEA December 2018; 49(4): 79–91.
- 23. Xu Ch., Ito K., Hayano K., Momoya Y. Combined effect of supported and unsupported sleepers on lateral ballast resistance in ballasted railway track. Transportation Geotechnics, 2023; 38. https://doi. org/10.1016/j.trgeo.2022.100913
- 24. Lundqvist, A., Dahlberg, T. Load impact on railway track due to unsupported sleepers. Proc. Inst. Mech. Eng. Part F J. Rail Rapid Transp. 2005; 219: 67–77. https://doi.org/10.1243/095440905X8790
- 25. Augustin, S., Gudehus, G., Huber, G., Schüunemann, A. Numerical model and laboratory tests on settlement of ballast track. In System Dynamics and

- Long-Term Behaviour of Railway Vehicles, Track and Subgrade; Popp, K., Schiehlen, W., Eds.; Springer: Berlin/Heidelberg, Germany, 2003; 317–336. https://doi.org/10.1007/978-3-540-45476-2 19
- 26. Sysyn M., Przybylowicz M., Nabochenko O., Liu J.. Mechanism of sleeper–ballast dynamic impact and residual settlements accumulation in zones with unsupported sleepers. Sustainability, 2021; 13: 7740. https://doi.org/10.3390/su13147740
- 27. Sadeghi J., Zakeri J-A., Kian A.R.T. Effect of unsupported sleepers on rail track dynamic behaviour. Sustainability 2021; 13(14): 7740; https://doi.org/10.3390/su13147740 (Proceedings of the Institution of Civil Engineers Transport 2018; 171(5): 286–298. https://doi.org/10.1680/jtran.16.00161
- Zhang S., Xiao X., Wen Z., Jin X. Effect of unsupported sleepers on wheel/rail normal load. Soil Dynamics and Earthquake Engineering 2008; 28: 662
 –673. https://doi.org/10.1016/j.soildyn.2007.08.006

- Liu D., Su Ch., Zhang D., Lan C. The influence of an unsupported sleeper on the vertical bearing characteristics of heavy-haul railway ballast. Materials 2024; 17: 1434. ttps://doi.org/10.3390/ma17061434
- 30. Droździel J., Sowiński B. Method of track vertical stiffness estimation based on experiment. The Archives of Transport, 2010; XXII(2): 153–162. https://doi.org/10.2478/v10174-010-0009-y
- 31. Sresakoolchai J., Kaewunruen S. Prognostics of unsupported railway sleepers and their severity diagnostics using machine learning. www.nature. com/scientificreports, 2022; 12: 6064. https://doi.org/10.1038/s41598-022-10062-w
- 32. https://www.zeiss.com/metrology/en/systems/optical-3d/3d-photogrammetry/pontos-live.html [Accessed: 11 Jun. 2025]
- 33. Eisenberger M., Yankelevsky D. Z. Exact stiffness matrix for beams on elastic foundation. Computers & Structures, 1985; 21(6).